Cancer Cell International

RESEARCH Open Access

USP24 promotes hepatocellular carcinoma progression by deubiquitinating and stabilizing YAP1

Huizhuang Shan[1*], Jiaguo Yuan[2], Luhua Xian[1], Wenmin Li[1], Yanfen Ge[1], Lei Zhang[1], Ting Lin[1], Mingwei Lan[1], Junru Liu[1], Yanfei Luo[1*], Yingli Wu[3*] and Xinhua Xiao[2*]

Abstract

Yes-associated protein 1 (YAP1) plays a pivotal role in promoting the progression of hepatocellular carcinoma (HCC). Emerging evidence shows that inducing YAP1 degradation represents a promising strategy. Here, we identified USP24 as a bona fide deubiquitinating enzyme for YAP1. USP24 directly interacts with and deubiquitinates YAP1, thereby stabilizing YAP1 protein levels. Clinically, USP24 was significantly upregulated in HCC tissues and correlated with poor patient prognosis. Depletion of USP24 significantly suppressed the proliferation of HCC cells in vitro, which could be rescued by restoration of YAP1. Consistent with these findings, USP24 knockdown inhibited tumor growth in a xenograft mouse model. Overall, our study reveals that the USP24/YAP1 axis plays a critical role in the malignant progression of HCC, thus providing rationale for potential therapeutic interventions for YAP1-driven HCC.

Keywords USP24, YAP1, HCC, Deubiquitinating enzyme, Proliferation

Introduction

Liver cancer, primarily in the form of hepatocellular carcinoma (HCC), is a leading cause of cancer-related death worldwide, ranking third in global mortality statistics [1]. In China, the impact is particularly significant, with 367,650 new cases and 316,540 deaths reported in 2022 [2]. The incidence rates in male are at least two to three times those in female regardless of race and geography, and this sex ratio is more pronounced in high-risk areas [3].The increasing global burden of HCC is attributed to the insidious onset and the limited efficacy of existing therapeutic strategies [4]. Sorafenib, a multi-target tyrosine kinase inhibitor, marks a milestone as the first approved systemic therapy for the treatment of unresectable HCC [5, 6]. However, recent advancements in immune checkpoint inhibitor-based combinations have reshaped the therapeutic landscape. The combination of atezolizumab (anti-PD-L1) and bevacizumab

*Correspondence:
Huizhuang Shan
shanhuizhuang@gdph.org.cn
Yanfei Luo
luoyanfei@gdph.org.cn
Yingli Wu
wuyingli@shsmu.edu.cn
Xinhua Xiao
xinhxiao@163.com
[1]Department of Clinical Laboratory Medicine, Guangdong Provincial People's Hospital (Guangdong Academy of Medical Sciences), Southern Medical University, Guangzhou, China
[2]Department of Hematology and Oncology, Guangzhou Women and Children's Medical Center, Guangzhou Medical University, Guangzhou, China
[3]Institute for Translational Medicine on Cell Fate and Disease, Shanghai Ninth People's Hospital, Key Laboratory of Cell Differentiation and Apoptosis of National Ministry of Education, Department of Pathophysiology, Shanghai Jiao Tong University School of Medicine, Shanghai, China

(anti-VEGF), supported by the landmark IMbrave150 trial (HR = 0.66 for overall survival), is now recognized as the first-line standard per international guidelines [7]. Additionally, the STRIDE regimen (single tremelimumab priming dose with durvalumab), validated in the phase III HIMALAYA trial (median OS: 16.4 months), has been approved as an alternative first-line option [8]. Tyrosine kinase inhibitors such as sorafenib and lenvatinib are currently reserved for patients ineligible for immunotherapy due to contraindications (e.g., active autoimmune disorders). Despite this progress, most patients undergoing therapy for HCC eventually develop resistance, leading to disease recurrence and metastasis, which adversely affects patient prognosis [9, 10]. Therefore, there is an urgent to discover new molecular markers associated with HCC and to develop effective treatment strategies.

The Hippo signaling pathway is a highly conserved tumor suppressor signaling pathway, composed of various protein kinases [11]. Yes-associated protein 1 (YAP1) is a downstream effector negatively regulated by the Hippo signaling pathway, primarily acting as a transcriptional co-activator. It can regulate the transcriptional activation of downstream proliferation-associated target genes, such as *CTGF*, *CYR61*, and *Birc5*, thereby controlling organ size, promoting cell proliferation, and inhibiting apoptosis [12–16]. As the main effector of the Hippo signaling pathway, YAP1 is mainly regulated by the key Hippo kinases, large tumor suppressor kinase 1/2 (LATS1/2). When the Hippo signaling pathway is activated, LATS1/2 are phosphorylated, which in turn phosphorylates YAP1. Phosphorylated YAP1 is retained in the cytoplasm, undergoes ubiquitination modification, and is ultimately transported to the proteasome for degradation [17]. It has been reported that aberrant activation of YAP1 is closely associated with the occurrence of various human cancers, including HCC, non-small cell lung cancer, breast cancer, colon cancer, and pancreatic cancer [18–20]. Overexpression of YAP1 can directly induce liver cancer formation in mice. Therefore, YAP1 is considered an important target for intervening in the malignant progression of HCC, and inhibiting the activity of YAP1 can effectively suppress the growth of tumor cells [21, 22]. However, YAP1 is difficult to be directly targeted by drugs, mainly due to its large protein-protein interaction interface and the lack of deep binding pocket. Here, we focus on deubiquitinating enzymes (DUBs), where catalytic inhibition has been proven to provide a new strategy for solving the undruggability of their substrates [23].

USP24 is one of the largest DUBs in the ubiquitin-specific protease (USP) family. By interacting with substrates and its deubiquitinating activity, USP24 participates in the regulation of vital cellular progress such as cell apoptosis, cell cycle control, and DNA damage repair [24]. It is noteworthy that USP24 plays an important role in several cancers, such as lung cancer, gastric carcinoma, neuroblastoma, and multiple myeloma [25–28]. More importantly, resent studies reported that miR-21-5p promotes sorafenib resistance and the progression of HCC by regulating the ubiquitination of SIRT7 through USP24 [29]. Another study clarified that USP24 facilitates the oncogenesis of HCC by deubiquitinating and stabilizing TRAF2 [30]. Given the key role of USP24 in cancer development, much attention has been paid to developing specific USP24 inhibitors for cancer therapy, such as USP24-i-101 [31]. Therefore, more studies are needed to deepen the understanding of new substrates and the regulation mechanism of USP24 in HCC, which contribute to facilitate the development of effective therapies.

In this study, we identified USP24 as a novel DUB for YAP1, which can bind to YAP1 and stabilizes it through deubiquitination, thereby enhancing the expression of YAP1 downstream target genes. Furthermore, we found that the expression of USP24 is overexpressed and positively correlates with YAP1 in HCC cells and tumor tissues, and high USP24 level predicts poor prognosis in patients with HCC. We also proved a novel mechanism for USP24's involvement in HCC cell proliferation via its regulation of YAP1. Thus, our study suggests that USP24 will be a promising therapeutic target for patients with HCC, which with sustained activation of YAP1 protein.

Materials and methods

Cell culture and transfection

The human normal liver cell line HL-7702, human HCC cell lines HepG2, Hep3B, LM3, and PLC/PRF/5, and human embryo kidney (HEK293T) cells were purchased from American Type Culture Collection (ATCC, Manassas, VA, USA). Human HCC cell lines, Huh-7, Bel-7402, and SMMC-7721 were obtained from the Cell Bank of the Type Culture Collection of the Chinese Academy of Sciences (Shanghai, China). MHCC97-H and MHCC97-L were kindly provided from Dr. Yang Ma (Shanghai Jiao Tong University School of Medicine, Shanghai, China). PLC/PRF/5 cells were cultured in MEM (BasalMedia, Shanghai, China) supplemented with 10% fetal bovine serum (FBS; Gemini, Woodland, CA, USA), penicillin (100 U/mL), and streptomycin (100 mg/mL). All other abovementioned cell lines were incubated in Dulbecco's Modified Eagle Medium (DMEM; BasalMedia, Shanghai, China) supplemented with 10% FBS, penicillin (100 U/mL), and streptomycin (100 mg/mL) at 37 °C under an atmosphere containing 5% CO_2. For transfection, HEK293T cells were transfected with plasmids using polyethyleneimine (PEI; Sigma-Aldrich, Louis, MO, USA) under the instructions of manufacturers.

Plasmids and reagents

The Myc-YAP1 and Myc-YAP1(S127A) were constructed by PCR and subsequent insertion of the corresponding fragment into pcDNA3.1 vector. The pcDNA3.1-USP24^{WT}-3×Flag (USP24 wild-type) or pcDNA3.1-USP24^{C1698A}-3×Flag (USP24 catalytic mutant) were purchased from Nanjing Jingmai Biotech Co., Ltd (Nanjing, China). HA-Ubiquitin was purchased from Tsingke Biotech Co., Ltd (Beijing, China). The USP24 shRNAs or the negative control were cloned into pGIPZ vector for stable cells establishment. The ORF of YAP1 was cloned into lentiviral vector pLVX-IRES-neo along with Flag-tag for overexpressing YAP1. The 8×GTIIC-luciferase plasmids were obtained from Addgene (Cambridge, MA, USA) and used according to the manufacturer's instructions. WP1130 (Degrasyn; TargetMol Chemicals Inc., Boston, MA, USA) and EOAI3402143 (TargetMol Chemicals Inc.) were maintained as 20 mM stock concentrations. MG132 and cycloheximide (CHX) were purchased from Selleck Chemicals, Inc. (Houston, TX, USA). Dimethyl-sulfeoxide (DMSO; Sigma-Aldrich) was used as a solvent and negative control.

RNA interference, lentivirus, and transfection

SiRNAs for transient transfection were designed and synthesized to downregulate the candidate USPs (CNV ≥ 2%). To produce lentivirus, the expression vector were transfected into HEK293T cells along with the packaging plasmids (pMD2.G and psPAX2). After 48 h, the viral supernatant was collected and filtered using 0.45 μm cellulose acetate filter (Millipore, Merck KGaA, Darmstadt, Germany). The Huh-7 and Bel-7402 cells were infected with supernatants containing virus particles in the presence of polybrene (8 μg/ml). After 48 h post infection, stably transfected cells were selected in medium containing 2 μg/mL puromycin (Sigma-Aldrich). The targeting sequences of shUSP24 were shown to be the following: shUSP24-1:5′-TGACAGTGAATAAAGATCA-3′; shUSP24-2:5′-CCACTACTATTCCTTCATT-3′.

Dual-luciferase reporter gene assay

The 8×GTIIC-luciferase plasmids, which harbors 8 TEADbinding sites and mutated TEAD binding sites, was utilized to indicate the transactivation YAP1. To screen DUBs for their effect on YAP1/TEAD4-driven luciferase activity, Bel-7402 cells were transfected with 8×GTIIC-luciferase plasmids, *renilla* luciferse, together with siRNA pools targeting candidate USPs (CNV ≥ 2%). After 48 h post-transfection, cells were lysed and assessed using luciferase activity assay. Firefly luciferase activity was normalized to the corresponding renilla luciferase activity by using the dual-luciferase reporter gene assay system (Promega, Madison, WI, USA).

RNA extraction, reverse transcription and quantitative real-time PCR (qRT-PCR)

Total RNA was extracted from Huh-7 and Bel-7402 cells using TRIzol reagent (Invitrogen, Carlsbad, CA, USA). HiScript III RT SuperMix for qPCR (+gDNA wiper) (Vazyme Biotech Co., Ltd, Nanjing, China) was used to reverse transcribe total RNA according to the manufacturer's instructions. The qRT-PCR assay was conducted using ChamQ Universal SYBR qPCR Master Mix (Vazyme Biotech Co., Ltd) in ABI 7900 Real-time PCR System (Applied Biosystems, Inc. Foster City, CA, USA). All relevant primers used in this study were synthesised by Sangon Biotech (Shanghai, China) and detailed primer sequences are shown in Table S1. Each test was run in three times, and the relative target mRNA level was calculated using $2^{-\Delta\Delta Ct}$ method. *β-actin* was used as the internal reference gene.

Western blotting and co-immunoprecipitation (Co-IP) assays

Western blotting analysis was performed as previously described [32]. Briefly, cells were harvested and lysed by 1× SDS lysis buffer. Equal amount of protein samples was loaded on 8% polyacrylamide gel (Vazyme Biotech Co., Ltd) and then transferred to nitrocellulose membrane (GVS Filter Technology, Bologna, Italy). The membrane was then blotted with specific primary antibodies against YAP1 (cat. no. 14074; 1:1000 dilution; Cell Signaling Technology, Inc., Boston, MA, USA), USP24 (cat. no. ab129064; 1:2000 dilution; Abcam, PLC., Cambridge, UK), Flag (cat. no. AE005; 1:1000 dilution; ABclonal Biotech Co., Ltd., Wuhan, China), Myc (cat. no. M047-3; 1:1000 dilution; MBL, Nagoya, Japan), HA (cat. no. 3724; 1:1000 dilution; Cell Signaling Technology) and β-Actin (cat. no.66009-1-lg; 1:10,000 dilution; ProteinTech Group, Inc., Chicago, Illinois, USA). After overnight incubation at 4℃, HRP-conjugated secondary antibodies (cat. no.SA00001-1 or SA00001-2; 1:10,000 dilution; ProteinTech) were applied and luminescence signals on membrane was visualized by a ChemiDoc Imaging System (Bio-Rad, Hercules, CA, USA).

Co-immunoprecipitation assays (Co-IP) were performed as previously described [33]. Briefly, cells were harvested and lysed in RIPA lysis buffer (50mM Tris, pH 7.4; 150mM NaCl; 1% Nonidet P-40; 0.5% sodium deoxycholate; 0.1% SDS) supplemented with protease inhibitor cocktail (Beyotime Biotech Co., Ltd. Shanghai, China) on a rotary shaker at 4 °C for 30 min. After centrifugation at 4 °C, 12,000 rpm for 15 min, the supernatants were incubated with indicated primary antibodies or IgG control on a rotary shaker at 4 °C overnight. Next day, Protein A/G Plus agarose beads (Beyotime) were added for additional 3 h. The beads were washed with the lysis buffer three times. Finally, the bound proteins were dissolved

in 2×SDS-PAGE loading buffer and analyzed by western blotting.

Ubiquitination assay

In order to assess the ubiquitination of YAP1 protein, HEK293T cells were transfected with indicated plasmids for 48 h, then treated with MG132 (10 μM) for 4 h before lysis. Cell lysates were subjected to immunoprecipitation assays as described above.

Immunofluorescence staining

HCC cells were fixed with 4% paraformaldehyde for 15 min at room temperature (RT). Then, fixed HCC cells were permeabilized with 0.5% Triton X-100 for 10 min at RT, and blocked with 5% bovine serum albumin (BSA; Sigma-Aldrich) in PBS for 1 h at RT. HCC cells were incubated with the indicated USP24 (cat. no. 13126-1-AP; 1:100 dilution; Proteintech) and YAP1 (cat. no. RT1664; 1:100 dilution; HUABIO, Hangzhou, China) primary antibodies overnight at 4 °C, followed by incubation with anti-rabbit iFluor™ 488 or anti-mouse iFluor™ 647 conjugates secondary antibody (cat. no. HA1121 or HA1127; 1:200 dilution; HUABIO) for 2 h at RT. Cell nuclei were counterstained with DAPI (Invitrogen). Confocal imaging was performed using a laser confocal microscope (LSM 900; Carl Zeiss, Jena, Germany).

Cell proliferation assays

Cell proliferation was assessed by trypan blue exclusion assay, colony formation assay and Cell Counting Kit-8 (CCK-8) assay. Bel-7402, Huh-7 and PLC/PRF/5 cells infected with indicated lentivirus were seeded 2×10^5 cells/well in 6-well plates. At the indicated time points (0, 2, 4, and 6 days), cells were suspended with 0.05% trypsin-EDTA and stained with trypan blue dye (0.4%). The unstained (viable) and stained (dead) cells were counted in an automated cell counter (Bio-Rad).

For the colony formation assay, lentivirus infected HCC cells were seeded $2–4 \times 10^3$/well in 6-well plates. Culture medium was changed every 3 days. Two weeks later, the cell clones were stained for 15 min with the solution containing 0.5% crystal violet (Beyotime) and 25% methanol, followed by rinsing with tap water three times to remove excess dye. The numbers of colonies were counted under microscope.

CCK-8 assay was conducted as previously described [34]. Briefly, lentivirus infected HCC cells (5×10^3 cells/well) were seeded in 96-well plates for indicated time points. To determine the cell viability of the cells, a 10 μL aliquot of CCK-8 solution (CK04; Dojindo Molecular Technologies, Inc., Kumamoto, Japan) was added in each well for an additional 4 h incubation. Optical density (OD) at 450 nm was then detected using a Synergy H4 Hybrid Microplate Reader (BioTek Instruments, Inc., Winooski, VT, USA).

Bioinformatic analysis

We analyzed the Cancer Genomics Atlas (TCGA) database by TIMER 2.0 (http://timer.cistrome.org/) to inve stigate the USP24 transcript level in different tumor tissues. Dataset of "Roessler Liver 2" from the Oncomine database (http://www.oncomine.org/) or TCGA-LIHC database from GEPIA platform were employed to analyze the differential expression of USP24 between primary HCC tumor tissues and non-tumor tissues. Kaplan-Meier curves for the correlation of USP24 expression with overall survival (OS) and diseases free interval (DFS) were obtained by an appropriate cutoff value using GEPIA (http://gepia.cancer-pku.cn/). For correlation ana lysis between USP24 and YAP1, data were performed by GEPIA (http://gepia.cancer-pku.cn/). We also analyzed RNA-seq expression data based on the tumor stages of patients with HCC obtained from TCGA-LIHC database, including 271 cases (Normal:40; Stage I:116; Stage II:56; Stage III:55; Stage IV:4). Gene expression analysis was conducted and visualized using the "ggplot2" package for R, after data normalization.

Tissue microarray and immunohistochemistry (IHC) analysis

Tissue microarray (cat. no. HLivH180Su30; Shanghai Outdo Biotech. Co., Ltd, Shanghai, China) containing 90 pairs of HCC tissues and their matched normal tissues were used to analyze the level of USP24 and YAP1. Patients with tissue flaking were excluded from the analysis (1 HCC tissue and 2 normal tissues for USP24; 5 HCC tissues and 6 normal tissues for YAP1). This resulted in 177 samples retained for USP24 analysis and 169 samples for YAP1 analysis. IHC staining was performed as previously described [35]. The following primary antibodies were used: USP24 (cat. no. 13126-1-AP; 1:500 dilution; Proteintech) and YAP1 (cat. no. 14074; 1:500 dilution; Cell Signaling Technology). The IHC staining intensity in the tissue microarray was scored as follows: no staining, 0; weak staining, 1; moderate staining, 2; and strong staining, 3. Samples with a score of 0 or 1 were classified as having low expression, while those with a score of 2 or 3 were classified as having high expression.

Animal experiments

Five-week-old female BALB/c nu/nu mice were purchased from Ruige biological technology Co., Ltd (Guangzhou, China) and housed under standard conditions. Briefly, the BALB/c nude mice were weight-stratified and randomly divided into two groups ($n = 6$ per group). 5×10^6 Bel-7402 cells (stably transfected with shNC or shUSP24-2) were mixed with matrigel (Corning,

Bedford, MA, USA) at a 1:1 ratio suspended in 100 μL PBS, and then injected subcutaneously into the right flanks of the mice. When the tumors became palpable, their sizes were monitored every 2 days and the tumor volumes were calculated using the standard formula: $V = a \times b^2/2$, where a and b are the length and the width of tumor, respectively. Tumors were measured by blinded operators using calipers, with analysis done independently before unblinding. At the end of the animal experiment on day 20, the tumors were isolated, photographed, and weighed. Then, the samples were fixed in 4% paraformaldehyde and prior to being embedded in paraffin for further study. All animal studies were approved by the Animal Ethics Committee at Southern Medical University (Guangzhou, China). This study complied with all relevant ethical regulations regarding animal research.

Statistical analysis

All graphs were generated using GraphPad Prism 8 software (GraphPad Software Inc., La Jolla, CA, USA). Data were obtained from at least three independent experiments and presented as mean ± standard deviation (SD). Data were analyzed using either Student's *t*-test (two-group comparison) or one-way ANOVA (more than two groups). *P* values less than 0.05 were considered statistically significant, and different levels were denoted as *, $P < 0.05$, **, $P < 0.01$, and ***, $P < 0.001$, respectively.

Results

Identification of USP24 as a regulator associated with the Hippo-YAP1 pathway in HCC

To discover the DUBs highly correlated with the activity of the Hippo-YAP1 pathway in HCC, we performed a DUB screen by analyzing gene copy number variants (CNVs) and monitoring YAP1-dependent transcriptional activity (Fig. S1A). We first analyzed the CNVs of 56 USPs in the TCGA database using cBioPortal, and found that USP21 showed the highest number of CNVs (Fig. 1A). Then, we downregulated the expression of the candidate USPs (CNV ≥ 2%) in the HCC cell line Bel-7402. The 8×GTIIC luciferase assay results showed that only USP24 but not USP21 inhibited the transcription activity driven by the YAP1/TEAD4 complex (Fig. 1B), indicating that USP24 plays a role in Hippo-YAP1 pathway activity in HCC cells. To further confirm the regulatory effects of USP24 in the Hippo-YAP1 signaling pathway, the Bel-7402, Huh-7 and PLC/PRF/5 cells were treated with WP1130, a pan-DUB inhibitor, to inhibit the USP24's DUB activity. The results showed that WP1130 could markedly reduce the protein expression of YAP1 (Fig. 1C and Fig. S1B). We also treated HCC cells with EOAI3402143, an alternative pan-DUB inhibitor targeting USP9X, USP24, and USP5, and observed significant YAP1 protein reduction (Fig. S1C-E). To exclude potential confounding effects of USP9X and USP5, we performed siRNA-mediated knockdown of these DUBs in Bel-7402 cells. The results demonstrated no alteration in YAP1 protein levels (Fig. S1F, G). These results collectively suggest that EOAI3402143 likely regulates YAP1 abundance primarily through USP24 inhibition. After the depletion of USP24 in Bel-7402, Huh-7 and PLC/PRF/5 cells by shRNAs treatment, a downregulation in the protein level of YAP1 was also observed (Fig. 1D and Fig. S1H). Interestingly, qRT-PCR analysis results further revealed that the downregulation of USP24 expression in HCC cells lowered the mRNA expression levels of YAP1 targeted genes, including *CTGF* (~ 50%; $P < 0.05$) and *CYR61* (~ 50%; $P < 0.05$), without affecting the mRNA level of *YAP1* (Fig. 1E), suggesting that USP24 might regulate the expression of YAP1 at the post-translational level.

Our results also showed that, after HEK293T cells were transfected with increasing amounts of the Flag-USP24 plasmid, the expression of YAP1 increased in a dose-dependent manner (Fig. 1F). Moreover, a cycloheximide (CHX) chase experiment indicated that the co-expression of Flag-USP24 could significantly prolong the half-life of exogenous Myc-tagged YAP1 compared to the negative control (Fig. 1G). In addition, Bel-7402 cells stably expressing control shRNA or USP24 shRNAs were treated with CHX, and the following CHX chase experiments showed that YAP1 protein was much more unstable in USP24-deficient cells (Fig. 1H). Collectively, these findings suggest that USP24 plays a role in Hippo-YAP1 pathway activity in HCC cells and stabilizes YAP1 expression.

USP24 interacts with YAP1

To assess the molecular mechanism through which USP24 regulates YAP1 expression, we first explored the interaction between USP24 and YAP1. Using a Co-IP assay, we examined the interactions between exogenous USP24 and exogenous YAP1 or between exogenous USP24 and endogenous YAP1, the results showed that USP24 and YAP1 were readily co-immunoprecipitated with each other (Fig. 2A, B). To investigate whether LATS1/2-mediated phosphorylation of YAP1 affects its binding to USP24, we co-expressed YAP1 phosphorylation-site mutants (YAP1-S127A) with USP24 in HEK293T cells and performed Co-IP assays. The results demonstrated that the phospho-deficient YAP1-S127A mutation enhanced USP24's binding (Fig. S2), suggesting phosphorylation negatively regulates this interaction. An interaction between endogenous USP24 and YAP1 was also validated in Bel-7402 and Huh-7 cells (Fig. 2C). To further demonstrate their interaction, the co-localization of USP24 and YAP1 in HCC cells was detected by immunofluorescence. As shown in Fig. 2D and Fig. S3A, USP24

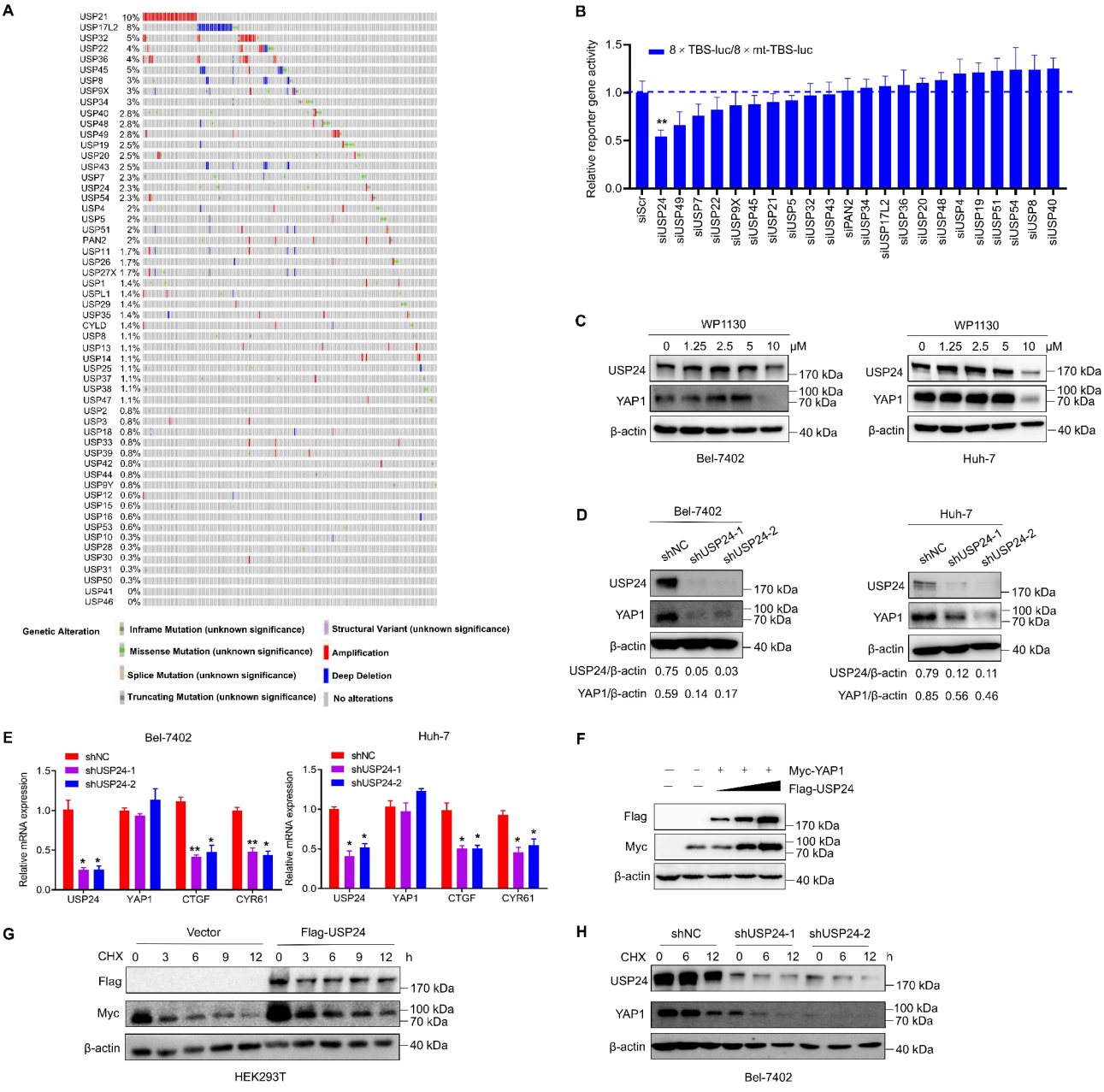

Fig. 1 Identification of USP24 as a regulator for YAP1 in HCC. **A** Analysis and generation of heat maps of CNV values of 56 USPs in the STAD dataset using cBioPortal. **B** After silencing USPs (CNV≥2%) in Bel-7402 cells, YAP1/TEAD4-driven transcriptional activity was accessed, and it is represented by the ratio of 8×GTIIC-luciferase activity with 8 TBSs to GTIIC luciferase activity with 8 mutant TBSs. **C** Bel-7402 and Huh-7 cells were treated with increasing concentrations of WP1130 for 12 h, and the indicated proteins were measured by western blotting. **D** USP24 was depleted by shRNAs (shUSP24-1 and shUSP24-2) in HCC cells and the indicated proteins were examined by western blotting. Control shRNA (shNC) was used as negative control. **E** qRT-PCR analysis of the indicated genes in Bel-7402 and Huh-7 cells with USP24 knockdown. **F** Increasing amounts of Flag-USP24 plasmids were co-transfected with Myc-YAP1 plasmid into HEK293T cells and the indicated proteins were examined by western blotting. **G** HEK293T cells were transfected with Flag-USP24 or vector plasmids. A CHX chase experiment was performed and Myc-tagged YAP1 protein was determined by western blotting (upper panel). The lower panel shows the relative protein amounts of different groups. **H** Bel-7402 cells stably expressing control shRNA or USP24 shRNAs were treated with or without CHX (20 mg/mL) and harvested at the indicated times, and indicated proteins was determined by western blotting (upper panel). The lower panel shows the relative protein amounts of different groups. Data are presented as mean ± SD, and *P* values were calculated using Student t test. $^{*}P < 0.05$ and $^{**}P < 0.01$

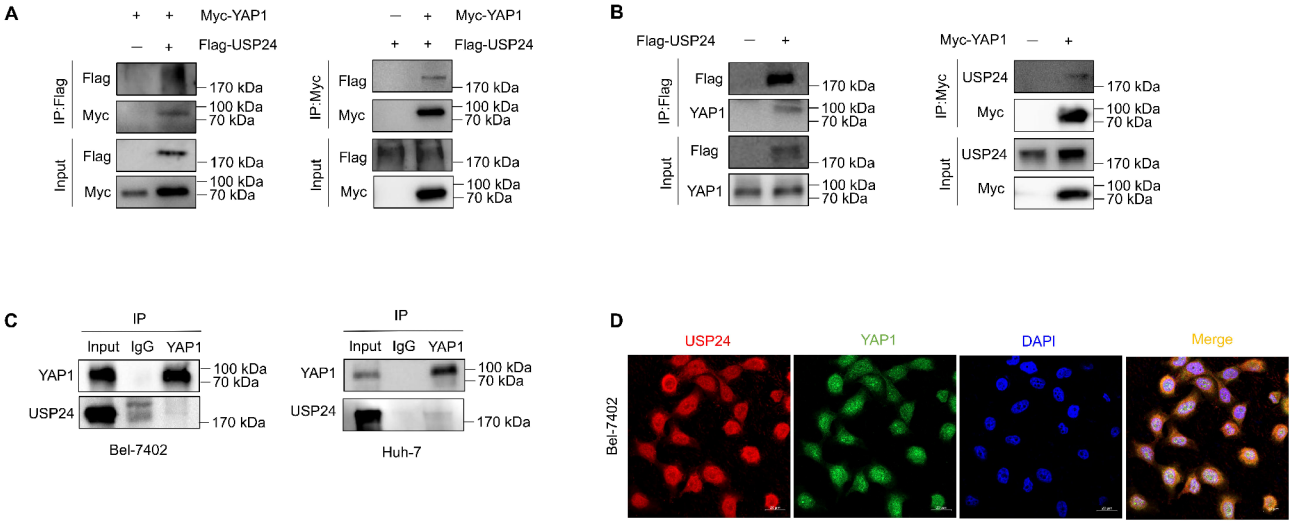

Fig. 2 USP24 interacts with YAP1. **A** HEK293T cells were transfected with plasmids encoding Flag-USP24 and/or Myc-YAP1. After 48 h of transfection, cell extracts were prepared and immunoprecipitated with anti-Flag or anti-Myc antibodies. The protein interactions were analyzed by western blotting. **B** HEK293T cells were transfected with plasmids encoding Flag-USP24 or Myc-YAP1. After 48 h of transfection, cell extracts were prepared and immunoprecipitated with anti-Flag or anti-Myc antibodies, and the indicated proteins were examined by western blotting. **C** Whole-cell lysates from Bel-7402 or Huh-7 cells were subjected to immunoprecipitation assays with a control IgG or an anti-YAP1 antibody. The immunoprecipitates were detected by western blotting. **D** Confocal microscopic analysis of USP24 and YAP1 subcellular localization. Bel-7402 cells were fixed and immunostained with antibodies against the indicated proteins. Representative images from biological triplicate experiments are shown. Scale bar, 20 μM

and YAP1 proteins were co-localized in the cytoplasm of Bel-7402 and Huh-7 cells. Owing to the absence of structural information on the interaction between USP24 and YAP1, we generated a complex structural model of the interaction between USP24 and YAP1 by using the AlphaFold3 server [36], which provided a structural view to understand the interactions between USP24 and YAP1. The model revealed that USP24's catalytic domain may interact with YAP1's N-terminal region (Fig. S3B). These data demonstrate that USP24 physically interacts with YAP1 in the cytoplasm of HCC cells.

USP24 deubiquitinates YAP1

It is well known that USP24 restrains the degradation of ubiquitinated proteins by removing ubiquitin chains from its substrates, hence we hypothesized that USP24 might stabilize YAP1 protein through deubiquitination. For this purpose, HEK293T cells were co-transfected with plasmids encoding HA-ubiquitin and Myc-YAP1 with or without wild-type USP24 ($USP24^{WT}$) or catalytically-inactive USP24 ($USP24^{C1698A}$). Ubiquitinated-YAP1 was immunoprecipitated and as illustrated in Fig. 3A, the co-expression of YAP1 with the $USP24^{WT}$, instead of the $USP24^{C1698A}$, decreased the protein levels of the ubiquitinated-YAP1. Consistently, the inhibition of USP24 by WP1130 apparently blocked the ability of USP24 to remove ubiquitin chains from YAP1 (Fig. 3B). Moreover, the HEK293T cells stably expressing shRNAs specifically against USP24 were co-transfected with plasmids encoding HA-ubiquitin and Myc-YAP1. The protein levels of ubiquitinated YAP1 increased after the knockdown of USP24 (Fig. 3C). Taken together, these results indicate that USP24 targets YAP1 for deubiquitination, supporting the hypothesize that YAP1 is a substrate for the deubiquitinating enzyme USP24.

USP24 is upregulated and associated with poor prognosis in HCC patients

To assess the USP24 expression in HCC, we first used the TCGA database to investigate the expression levels of USP24 in various tumor tissues, it was found that USP24 was highly expressed in LIHC tissues (Fig. 4A). The data from Oncomine database also indicated the upregulation of USP24 in liver cancer tissues compared to normal ones (Fig. 4B). Additionally, GEPIA platform results from TCGA-LIHC data showed significant upregulation of USP24 mRNA expression level in LIHC tissues compared to normal tissues (Fig. 4C). We also observed that the expression of USP24 was correlated with certain clinicopathological features in patients with HCC. As shown in Fig. 4D, upregulated expression of USP24 was prominently associated with different tumor stages of HCC. Survival curves demonstrated that a higher transcriptional level of USP24 was significantly correlated with shorter OS (HR = 1.7, $P = 0.0021$) and DFS (HR = 1.9, $P < 0.001$) in patients with HCC (Fig. 4E). The Human Protein Atlas was also analyzed, revealing consistent upregulation of USP24 in HCC tissues (Fig. 4F). Altogether, these results demonstrate that USP24 levels are significantly elevated in HCC and that its expression

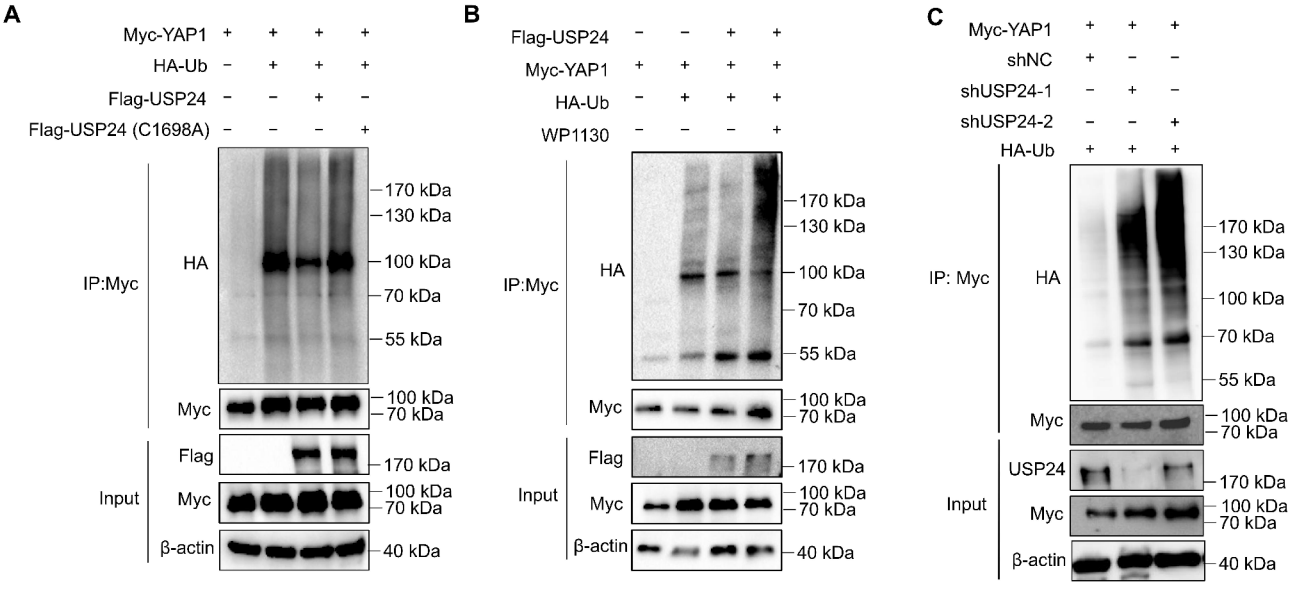

Fig. 3 USP24 deubiquitinates YAP1. **A** HEK293T cells were co-transfected with the specified plasmids. After 48 h of transfection, cell extracts were prepared for immunoprecipitation assays with anti-Myc followed by western blotting with anti-HA antibody. **B** HEK293T cells were co-transfected with the indicated plasmids, treated with or without WP1130 (10 μM) for 8 h before cells were harvested. Further, cellular extracts were prepared for immunoprecipitation assays with anti-Myc followed by western blotting with anti-HA antibody. **C** HEK293T cells stably expressed shRNAs specifically against USP24 and co-transfected with the indicated plasmids. Cellular extracts were immunoprecipitated with anti-Myc followed by western blotting with anti-HA antibody

also plays an important role in predicting the clinical outcomes of patients with HCC.

USP24 is upregulated in tumor samples and correlates with the protein levels of YAP1

Next, we sought to confirm the clinical significance of USP24 and its correlation with YAP1 in HCC. Spearman correlation analyses using TCGA database showed that an apparent positive correlation was detected between the expression level of USP24 and YAP1 or those of YAP1 target genes (*CTGF* and *CYR61*) in patients with HCC (Fig. 5A and Fig. S4 A, B). Also, western blotting analysis revealed that USP24 was highly expressed in HCC cell lines compared with the normal liver cell line HL7702, and USP24 protein level was highly associated with YAP1 protein level in HCC cell lines (Fig. 5B). Furthermore, we evaluated USP24 and YAP1 expression in microarray tissues from 90 HCC tissues and matched normal tissues using IHC staining (Fig. 5C and Fig. S5A). Most tumor specimens expressed high volume of USP24 and YAP1 (Fig. 5D, E and Fig. S5B). The relationship between USP24 expression and clinicopathological characteristics was also investigated (Table S2). The results showed that increased USP24 expression was significantly correlated with Grade ($P<0.001$), and TNM ($P=0.015$) in HCC tissues. Moreover, we utilized the Kaplan-Meier analysis to assess the correlation between USP24 expression levels and survival in the HCC tissue cohort. The results showed that upregulation of USP24 was associated with poor prognosis (Fig. S5C). Importantly, a statistically significant positive correlation was found between USP24 and YAP1 levels (Fig. S5D, $r=0.4756$, $P<0.001$). Overall, these observations indicate that the expression levels of USP24 in HCC tissues are high and correlated with the protein levels of YAP1.

USP24 regulates HCC cell proliferation in vitro and in vivo

To determine the biological role of USP24 in HCC, USP24 was silenced by shRNAs in HCC cells, and subjected to in vitro experiments. As depicted in Fig. 6A, B, knockdown of USP24 significantly suppressed cell proliferation by approximately 50% in Bel-7402 cells ($P<0.01$), 33% in Huh-7 cells ($P<0.01$) and 59% in PLC/PRF/5 cells ($P<0.001$). Similarly, knockdown of USP24 inhibited the colony formation by approximately 39% in Bel-7402 cells ($P<0.05$), 49% in Huh-7 cells ($P<0.05$) and 77% in PLC/PRF/5 cells ($P<0.001$) (Fig. 6C, D). Importantly, re-expression of YAP1 in USP24-depleted cells partially rescued USP24 depletion-induced inhibition, reducing cell proliferation from ~45–10% inhibition in Bel-7402 cells ($P<0.01$), from ~45–7% in Huh-7 cells ($P<0.01$), and from ~53–10% in PLC/PRF/5 cells ($P<0.001$) (Fig. 6E), while colony formation inhibition decreased from ~75–6% in Huh-7 cells ($P<0.001$) and from ~70–28% in PLC/PRF/5 cells ($P<0.001$) (Fig. 6F, G).

To investigate whether USP24 knockdown suppressed the tumorigenesis of HCC cells in vivo, we injected Bel-7402 cells which were stably knockdown USP24

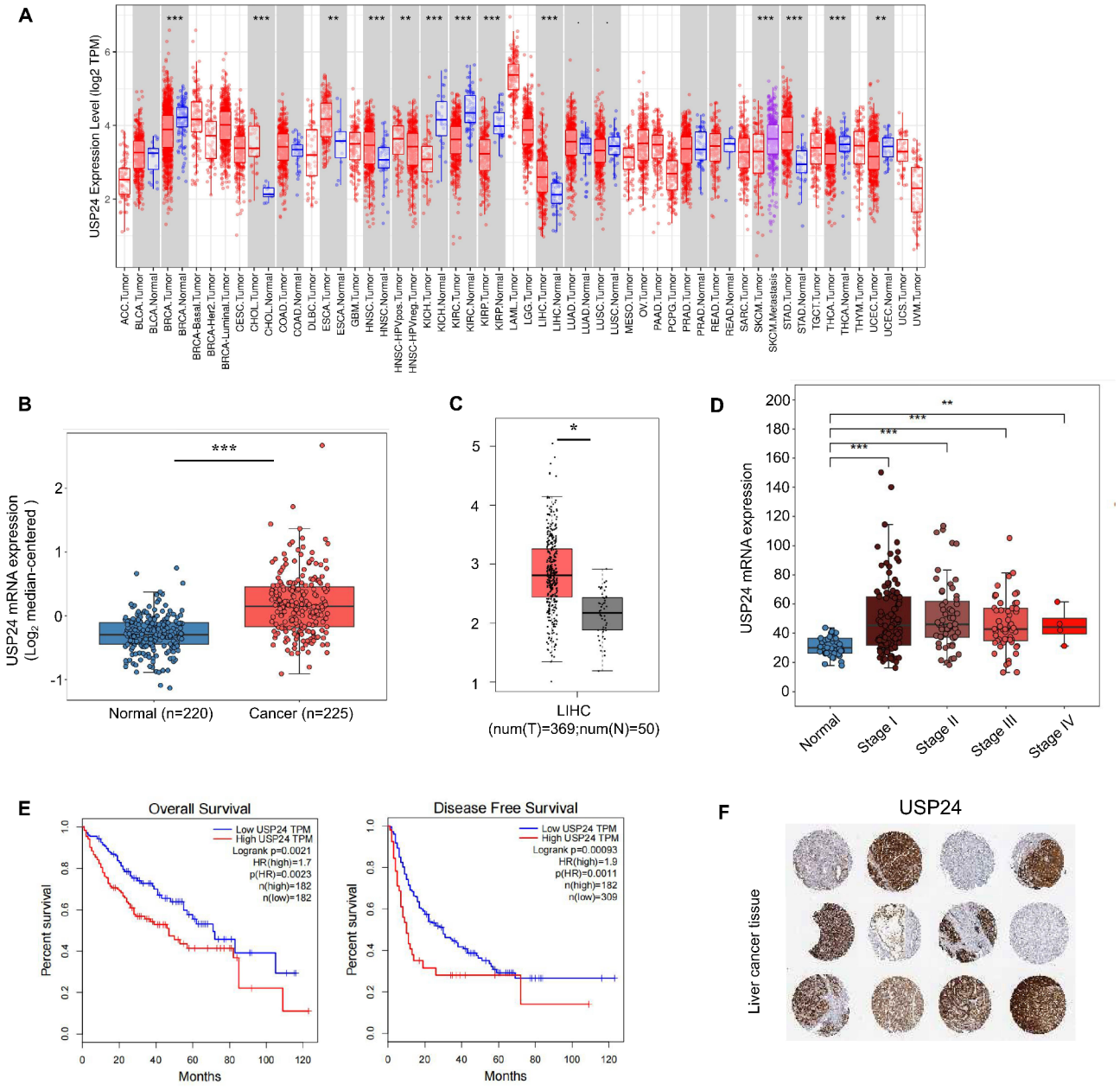

Fig. 4 USP24 is upregulated and associated with a poor prognosis in HCC. **A** USP24 mRNA expression level in different tumor tissues and non-tumor tissues from TCGA database was detected by TIMER 2.0 (http://timer.cistrome.org/). The red dots represent tumor tissues, while the blue dots represent normal tissues. **B** Analysis of TCGA liver cancer (Roessler Liver 2) from Oncomine database concerning the expression of USP24 in normal liver tissues and HCC tumor tissues. Data are presented by box plots. Fold change, *P* values (determined by Student's *t*-test), and sample size are shown. **C** Comparison of the USP24 mRNA expression level in the TCGA-LIHC database on the GEPIA platform. **D** Analysis of the USP24 mRNA expression level based on the tumor stages in HCC tissues according the TCGA-LIHC database. **E** Prognostic survival analysis of the overall survival (OS) or disease-free survival (DFS) for *USP24* gene from TCGA in HCC patients, using the GEPIA platform. The log-rank $P < 0.05$ is considered as a statistically significant value. The red and blue lines represent high and low expressions of *USP24* gene. **F** Expression of USP24 in patients with HCC patients was generally high. The representative IHC images were from the Human Protein Atlas database ($n = 12$). $^{*}P < 0.05$, $^{**}P < 0.01$, and $^{***}P < 0.001$

(shUSP24-2) or the negative control (shNC) into the subcutaneous of the nude mice. The results indicated that USP24 knockdown significantly decreased tumor volume by 67% ($P < 0.001$) and reduced tumor weight by 43% ($P < 0.001$) relative to the shNC control group (Fig. 6H, I). HE staining validated that all tumors were solid tumors (Fig. 6J). IHC staining analysis showed that shUSP24-2 group has lower percentages of proliferative cells, higher percentages of apoptotic cells, and lower level of YAP1 protein (Fig. 6J). These findings corroborate the notion that the regulatory effects on YAP1 are critical for USP24, which plays an oncogenic role in HCC cells.

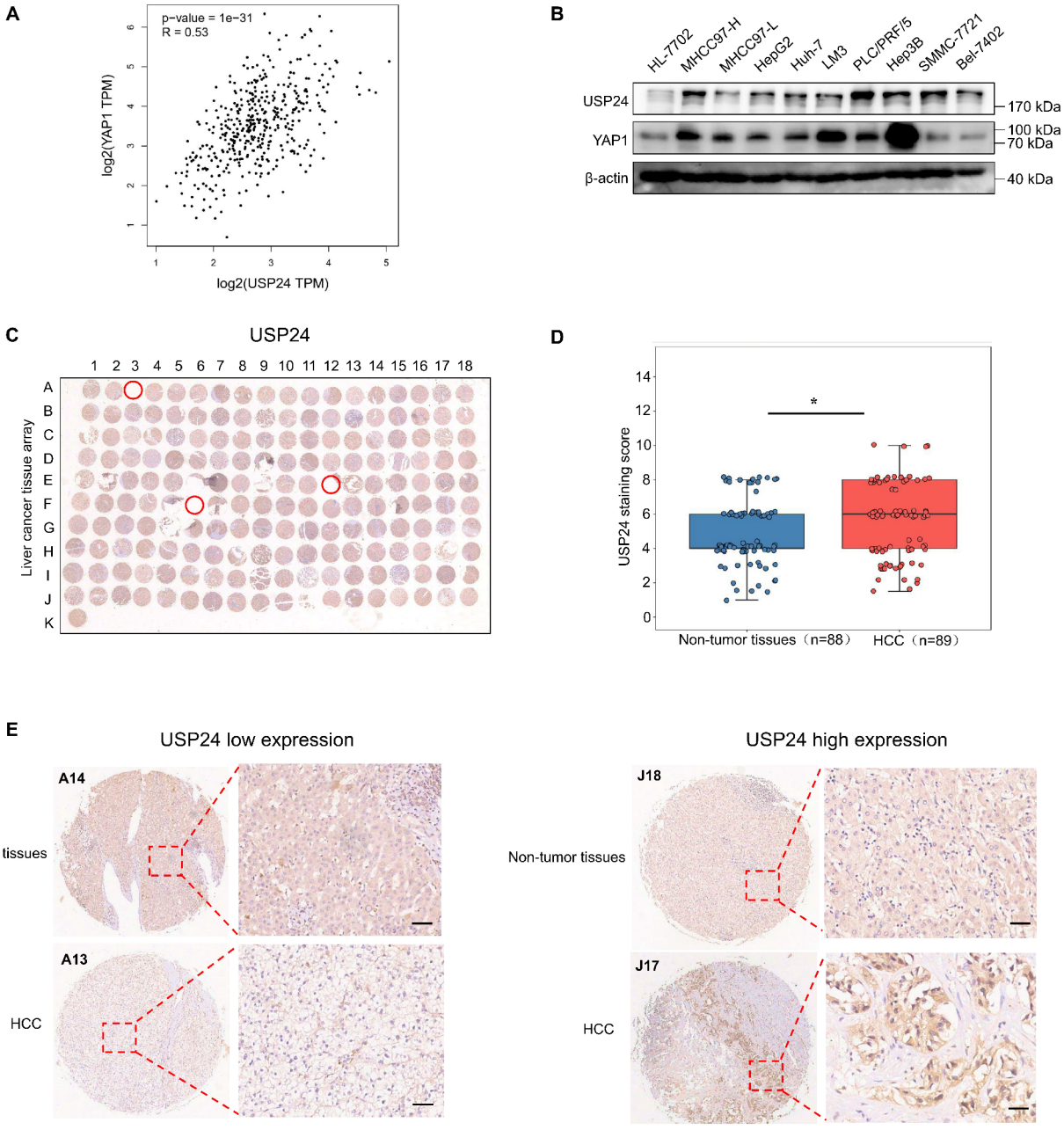

Fig. 5 USP24 is upregulated in tumor samples and correlates with the protein levels of YAP1. **A** Scatter plots showing the correlations between the USP24 expression level and YAP1 expression level in HCC patients by Spearman correlation analyses using GEPIA platform from TCGA database. **B** The USP24 and YAP1 protein level in various HCC cell lines were determined by western blotting. **C** Overall staining of USP24 in the tissue microarray. The microarray contained 90 pairs of HCC tissues and 90 matched normal tissues, and the detached spots (red circles) were excluded, which including 1 HCC tissue and 2 normal tissues, leaving 177 samples retained for analysis. **D** The USP24 staining score of HCC tissues ($n=89$) and matched normal tissues ($n=88$). **E** Representative IHC images of USP24 expression in HCC tissues and matched normal tissues. Scale bar, 50 μM. $^{*}P<0.05$

Discussion

HCC is the third leading cause of cancer deaths [37]. The lack of intervention targets remains an elusive, yet critical challenge in the discovery of therapeutic drugs for HCC. Accumulating evidence suggests that controlling the stability of YAP1 represents as a new approach to regulate the Hippo signaling pathway in HCC is attracting more attention. In this study, we demonstrate that inducing degradation of YAP1 by inhibiting USP24 is a promising strategy to combat HCC.

YAP1 is a critical downstream effector of the Hippo signaling pathway that play important oncogenic roles in human cancers, particularly in HCC [38–40]. Importantly, the expression of YAP1 in liver cancer stem cells

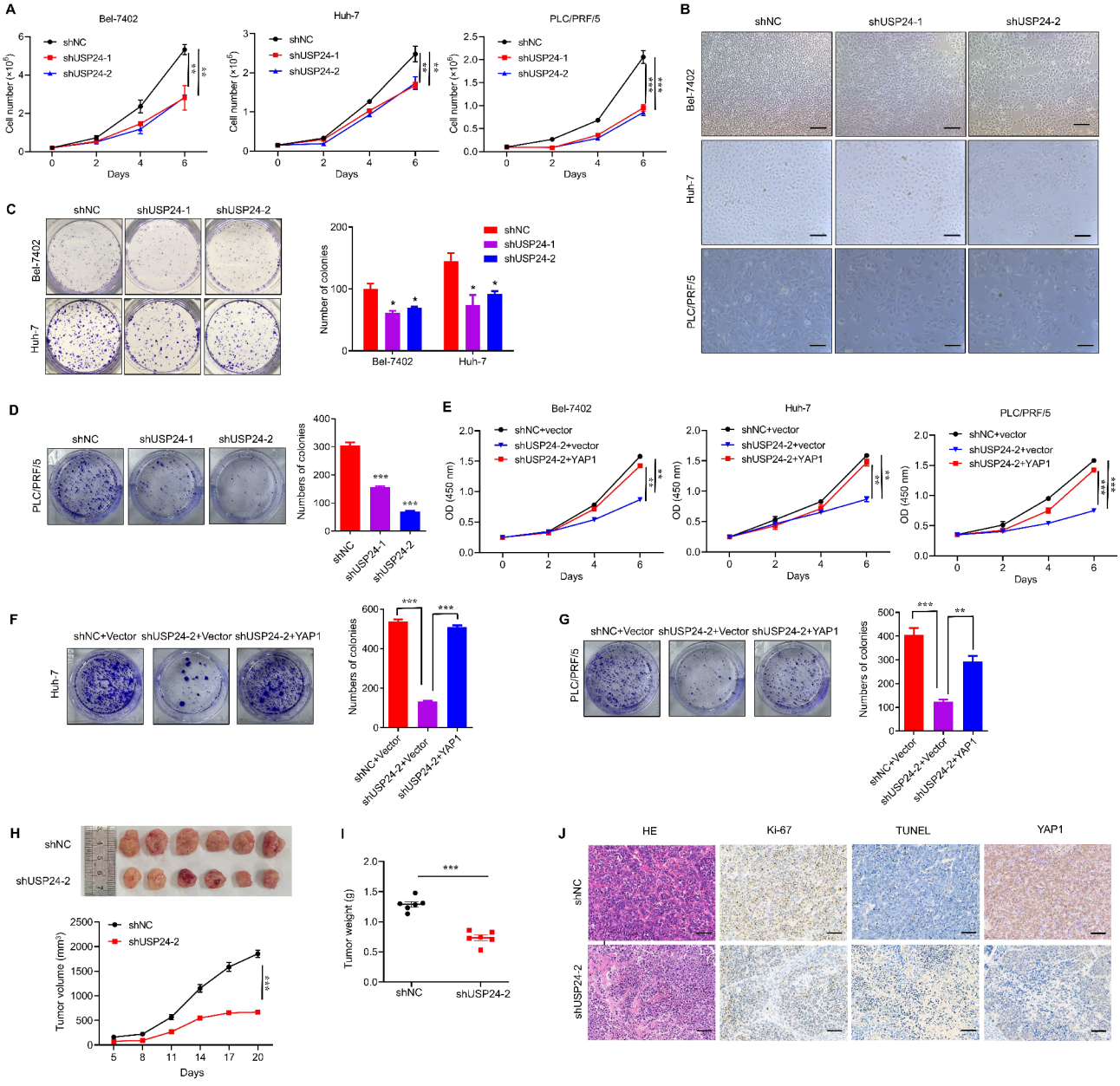

Fig. 6 USP24 regulates HCC cell proliferation in vitro and *in vivo*.**A** Bel-7402, Huh-7, or PLC/PRF/5 cells were infected with control shRNA or USP24 shRNAs, and cell proliferation was monitored by trypan blue exclusion assay. **B** Cell morphology (96 h) was captured under the microscope. Original magnification, ×200. **C** Bel-7402 or Huh-7 cells were transfected with the indicated plasmids and seeded into 6-well plates at a density of 2000 cells/well. After 14 days, colony formation was detected by crystal violet staining. **D** PLC/PRF/5 cells were transfected with the indicated plasmids and seeded into 6-well plates at a density of 4000 cells/well. After 14 days, colony formation was detected by crystal violet staining. **E** HCC cells were infected with either shCtrl + vector, shUSP24-2 + vector, or shUSP24-2 + YAP1, and cell proliferation was monitored by CCK-8 assay. **F**, **G** Huh-7 (**F**) and PLC/PRF/5 (**G**) cells were infected with either shCtrl + vector, shUSP24-2 + vector, or shUSP24-2 + YAP1, and cell proliferation was monitored by colony formation assay. **H**, **I** Bel-7402 cells stably transfected with either shNC or shUSP24-2 were subcutaneously injected into BALB/c nude mice ($n = 6$ for each group) to establish an HCC xenograft mouse model. After 20 days, tumors from 12 of the mice were extracted and photographed. Tumor images (**H**, upper panel), tumor volume (**H**, lower panel) and weight (**I**) were assessed. **J** Expression patterns of Ki-67, TUNEL and YAP1 were examined by IHC analysis in the xenograft tumors of each group, Scale bar, 20 μM. Data are presented as mean ± SD, and *P* values were calculated using Student t test. $^{*}P < 0.05$, $^{**}P < 0.01$, and $^{***}P < 0.001$

(LCSCs) is significantly increased, and the levels of YAP1 and YAP1-TEAD are positively correlated with the expression of stemness markers (such as NANOG, OCT-3/4, CD133), and are associated with the severity of liver cancer [41]. Suppressing the aberrant expression of YAP1 is therefore essential to alleviate tumor progression. However, different from that of protein kinases, YAP1 is technically challenging to be directly targeted.

An alternative strategy is to inducing the degradation of these transcription co-activators. Recently studies revealed that translational modifications, such as ubiquitination, is important in preventing YAP1 over-activation. Ubiquitination is a reversible process, and removal of ubiquitin from proteins is mediated by DUBs. Several researchers made effort to identify critical DUBs in stabilizing YAP1 protein that promotes tumor progression. For example, USP49 and OTUB1 were found to have the ability to maintain the stability of YAP1 through their interaction with YAP1, thus promoting gastric cancer cell proliferation, and metastasis [42, 43]. USP47 has been shown to be involved in the pathogenesis of colorectal cancer through deubiquitination and stabilization of YAP1 [44]. Moreover, Hong et al. identified USP10 as a novel deubiquitinating mediator that stabilizes YAP/TAZ in HCC and enhances downstream oncogenic response [45]. In our study, our candidate USPs (CNV ≥ 2%) in the HCC were not including USP10, and the screening identified that the downregulation of USP24 expression significantly inhibited the transcriptional activity of YAP1/TEAD4. The interaction between USP24 and YAP1 was also confirmed to stabilize YAP1 expression through deubiquitination and activation of the downstream target genes, such as *CTGF* and *CYR61*. These findings suggest that USP24 is a novel YAP1-interacting DUB. However, as this a small scale of screening (compared to the total 100 DUBs, only 22 of them were used in our test), we don't rule out other DUBs, such as USP10, may be also involved in the regulation of YAP1 stability in HCC. We also observed that phospho-deficient YAP1-S127A mutation enhanced USP24's binding, suggesting phosphorylation negatively regulates their interaction. The crosstalk between these post-translational modifications in controlling YAP1 stabilization requires further investigation.

USP24, as a ubiquitin-specific protease, plays different roles in tumorigenesis and cancer progression, and the pro-tumorigenic or anti-tumorigenic function of USP24 was largely depended on its substrates in the specific cellular context of cancer models. Previous study have shown that USP24 inhibits the progression of neuroblastoma by stabilizing CRMP2 [27]. In more types of cancer, USP24 has been found to have oncogenic functions. Our laboratory's previous study reported that USP24 plays an important role in the survival of T-cell acute lymphoblastic leukemia (T-ALL) cells and targeting USP24-Mcl-1 axis may represent a novel strategy in the treatment of T-ALL [46]. A recent publication found that USP24 accelerates aerobic glycolysis and tumor progression in gastric carcinoma through stabilizing PLK1 to activate NOTCH1 [28]. In this study, we explored the biological functions of USP24 in HCC models. By analyzing the database and combining the IHC staining analysis results of tissue microarrays, it was found that USP24 was highly expressed in HCC tissues. High expression level of USP24 was closely related to the poor prognosis in HCC patients. In addition, we also found that USP24 promoted cell proliferation and tumor growth of HCC in vitro and in vivo. During our research process, another study clarified that USP24 facilitates the oncogenesis of HCC by deubiquitinating and stabilizing TRAF2 [30]. However, Cao et al. suggested that USP24 plays an important role in preventing HCC progression through regulating autophagy-dependent ferroptosis by decreasing Beclin1 ubiquitination [47]. These seemingly contradicting conclusions drawn from independent studies may stem from: (1) different cellular contexts of the HCC cells - the tumor-suppressive function was observed in ferroptosis-sensitive HCC cell lines under oxidative stress conditions, whereas the oncogenic role was demonstrated in proliferating HCC cells; (2) distinct molecular mechanisms-USP24 may exert opposing effects through different substrates; (3) partial differences in experimental design. Moreover, due to the introduction of HCC patients' specimens and comprehensive TCGA database analyses in our study, we encouraged to conclude that USP24 indeed plays a crucial pro-tumorigenic role in HCC patients. More importantly, to the best of our knowledge, we proved for the first time that USP24 could regulate the stability of YAP1 in HCC cells. Unlike the importance of TRAF2 in HCC [30], a growing body of evidence suggests that approximately 60% of human liver cancer was associated with increased YAP1 activity [48], thus the regulatory mechanism of USP24 related to YAP1 protein will have a strong promoting effect on HCC cells. Therefore, targeting USP24 rather than inhibiting its enzyme activity may be potentially beneficial for combating "undruggable" of YAP1 in HCC.

Several limitations of this study should be noted. Althrough our subcutaneous xenograft model demonstated USP24's tumor-promoting effects, we acknowledge that this system lacks the native hepatic microenvironment present in orthotopic models. Recent studies demonstrate that liver-specific factors including Kupffer cells, hepatic stellate cells, and unique extracellular matrix components can significantly influence HCC progression and drug responses [49]. Particularly for YAP1/TAZ signaling which is known to be mechanosensitive, the soft subcutaneous niche may underestimate microenvironmental regulation [50]. Future studies employing intrahepatic implantation or patient-derived orthotopic xenografts (PDOX) will be essential to validate these findings in more physiologically relevant contexts. In addition, HCC is characterized by marked male predominance in incidence, yet most preclinical studies overlook potential sex differences in YAP1 signaling. Our study was conducted exclusively in female mice, and future

investigations using male mice will be required to validate the generalizability of our findings.

In summary, the current study shows that USP24 is an important protein that facilitates HCC progression. We identified that USP24 drives HCC progression by stabilizing YAP1 through direct interaction and deubiquitination, leading to constitutive activation of YAP1 downstream targets. Our findings indicate that USP24 may act as a novel biomarker for predicting prognosis and may present a therapeutic opportunity for HCC.

Supplementary Information

The online version contains supplementary material available at https://doi.org/10.1186/s12935-025-03796-w.

Supplementary Material 1

Supplementary Material 2

Acknowledgements
We acknowledge the prof. Yanhui Xu (Fudan university, Shanghai, China) for providing pLVX-IRES-neo-Flag-YAP1 plasmid.

Author contributions
H. Shan, X. Xiao, Y. Wu and Y. Luo elaborated the initial experimental design; H. Shan and X. Xiao performed the experiments; J. Yuan, L. Xian, W. Li, Y. Ge, L. Zhang, T. Lin, M. Lan and J. Liu conducted the data analysis; H. Shan and X. Xiao wrote the manuscript; H. Shan, X. Xiao, Y. Wu and Y. Luo reviewed the final manuscript.

Funding
This study was supported by grants from the National Natural Science Foundation of China (82200118, 82170145, 82470152), Guangdong Basic and Applied Basic Research Foundation (2024A1515012834), NSFC Incubation Project of Guangdong Provincial People's Hospital (KY0120220038).

Data availability
Publicly available datasets were analyzed in this study. These data can be found at https://portal.gdc.cancer.gov/.

Declarations

Ethics approval and consent to participate
All animal experiments were approved by The Animal Care & Welfare Committee of Guangdong Provincial People's Hospital (Guangdong Academy of Medical Sciences), Southern Medical University.

Consent for publication
Not applicable.

Competing interests
The authors declare no competing interests.

Received: 29 December 2024 / Accepted: 21 April 2025
Published online: 26 April 2025

References

1. Ducreux M, Abou-Alfa GK, Bekaii-Saab T, Berlin J, Cervantes A, de Baere T, Eng C, Galle P, Gill S, Gruenberger T, et al. The management of hepatocellular carcinoma. Current expert opinion and recommendations derived from the 24th ESMO/World Congress on Gastrointestinal cancer, Barcelona, 2022. ESMO Open. 2023;8(3):101567.
2. Ferlay J, Ervik M, Lam F, Laversanne M, Colombet M, Mery L, Piñeros M, Znaor A, Soerjomataram I, Bray F. (2024). Global Cancer Observatory: Cancer Today. Lyon, France: International Agency for Research on Cancer. Available at https://gco.iarc.fr/today. Accessed 08-02-2024.
3. Siegel RL, Kratzer TB, Giaquinto AN, Sung H, Jemal A. Cancer statistics, 2025. CA Cancer J Clin. 2025;75(1):10–45.
4. Llovet JM, Ricci S, Mazzaferro V, Hilgard P, Gane E, Blanc JF, de Oliveira AC, Santoro A, Raoul JL, Forner A, et al. Sorafenib in advanced hepatocellular carcinoma. N Engl J Med. 2008;359(4):378–90.
5. Llovet JM, Pena CE, Lathia CD, Shan M, Meinhardt G, Bruix J, Group SIS. Plasma biomarkers as predictors of outcome in patients with advanced hepatocellular carcinoma. Clin Cancer Res. 2012;18(8):2290–300.
6. Finn RS, Zhu AX, Farah W, Almasri J, Zaiem F, Prokop LJ, Murad MH, Mohammed K. Therapies for advanced stage hepatocellular carcinoma with macrovascular invasion or metastatic disease: A systematic review and meta-analysis. Hepatology. 2018;67(1):422–35.
7. Finn RS, Qin S, Ikeda M, Galle PR, Ducreux M, Kim TY, Kudo M, Breder V, Merle P, Kaseb AO, et al. Atezolizumab plus bevacizumab in unresectable hepatocellular carcinoma. N Engl J Med. 2020;382(20):1894–905.
8. Abou-Alfa GK, Lau G, Kudo M, Chan SL, Kelley RK, Furuse J, Sukeepaisarnjaroen W, Kang YK, Van Dao T, De Toni EN, et al. Tremelimumab plus durvalumab in unresectable hepatocellular carcinoma. NEJM Evid. 2022;1(8):EVIDoa2100070.
9. He AR, Goldenberg AS. Treating hepatocellular carcinoma progression following first-line Sorafenib: therapeutic options and clinical observations. Th Adv Gastroenterol. 2013;6(6):447–58.
10. Yang X, Yang C, Zhang S, Geng H, Zhu AX, Bernards R, Qin W, Fan J, Wang C, Gao Q. Precision treatment in advanced hepatocellular carcinoma. Cancer Cell. 2024;42(2):180–97.
11. Harvey KF, Zhang X, Thomas DM. The Hippo pathway and human cancer. Nat Rev Cancer. 2013;13(4):246–57.
12. Levy D, Adamovich Y, Reuven N, Shaul Y. Yap1 phosphorylation by c-Abl is a critical step in selective activation of proapoptotic genes in response to DNA damage. Mol Cell. 2008;29(3):350–61.
13. Tomlinson V, Gudmundsdottir K, Luong P, Leung KY, Knebel A, Basu S. JNK phosphorylates Yes-associated protein (YAP) to regulate apoptosis. Cell Death Dis. 2010;1(2):e29.
14. Rosenbluh J, Nijhawan D, Cox AG, Li X, Neal JT, Schafer EJ, Zack TI, Wang X, Tsherniak A, Schinzel AC, et al. beta-Catenin-driven cancers require a YAP1 transcriptional complex for survival and tumorigenesis. Cell. 2012;151(7):1457–73.
15. Yang S, Zhang L, Liu M, Chong R, Ding SJ, Chen Y, Dong J. CDK1 phosphorylation of YAP promotes mitotic defects and cell motility and is essential for neoplastic transformation. Cancer Res. 2013;73(22):6722–33.
16. Zhang L, Tang F, Terracciano L, Hynx D, Kohler R, Bichet S, Hess D, Cron P, Hemmings BA, Hergovich A, et al. NDR functions as a physiological YAP1 kinase in the intestinal epithelium. Curr Biol. 2015;25(3):296–305.
17. Zhao B, Li L, Tumaneng K, Wang CY, Guan KL. A coordinated phosphorylation by Lats and CK1 regulates YAP stability through SCF(beta-TRCP). Genes Dev. 2010;24(1):72–85.
18. Wang S, Xie F, Chu F, Zhang Z, Yang B, Dai T, Gao L, Wang L, Ling L, Jia J, et al. YAP antagonizes innate antiviral immunity and is targeted for lysosomal degradation through IKKvarepsilon-mediated phosphorylation. Nat Immunol. 2017;18(7):733–43.
19. Wang T, Mao B, Cheng C, Zou Z, Gao J, Yang Y, Lei T, Qi X, Yuan Z, Xu W, et al. YAP promotes breast cancer metastasis by repressing growth differentiation factor-15. Biochim Biophys Acta Mol Basis Dis. 2018;1864(5 Pt A):1744–53.
20. Chen YA, Lu CY, Cheng TY, Pan SH, Chen HF, Chang NS. WW Domain-Containing proteins YAP and TAZ in the Hippo pathway as key regulators in stemness maintenance, tissue homeostasis, and tumorigenesis. Front Oncol. 2019;9:60.
21. Zhou TY, Zhuang LH, Hu Y, Zhou YL, Lin WK, Wang DD, Wan ZQ, Chang LL, Chen Y, Ying MD, et al. Inactivation of hypoxia-induced YAP by Statins overcomes hypoxic resistance Tosorafenib in hepatocellular carcinoma cells. Sci Rep. 2016;6:30483.
22. Zhu H, Wang DD, Yuan T, Yan FJ, Zeng CM, Dai XY, Chen ZB, Chen Y, Zhou T, Fan GH, et al. Multikinase inhibitor CT-707 targets liver Cancer by interrupting the Hypoxia-Activated IGF-1R-YAP Axis. Cancer Res. 2018;78(14):3995–4006.
23. Harrigan JA, Jacq X, Martin NM, Jackson SP. Deubiquitylating enzymes and drug discovery: emerging opportunities. Nat Rev Drug Discov. 2018;17(1):57–78.
24. Song X, Xia B, Gao X, Liu X, Lv H, Wang S, Xiao Q, Luo H. Related cellular signaling and consequent pathophysiological outcomes of ubiquitin specific protease 24. Life Sci. 2024;342:122512.

25. Peterson LF, Sun H, Liu Y, Potu H, Kandarpa M, Ermann M, Courtney SM, Young M, Showalter HD, Sun D, et al. Targeting deubiquitinase activity with a novel small-molecule inhibitor as therapy for B-cell malignancies. Blood. 2015;125(23):3588–97.
26. Wang YC, Wu YS, Hung CY, Wang SA, Young MJ, Hsu TI, Hung JJ. USP24 induces IL-6 in tumor-associated microenvironment by stabilizing p300 and beta-TrCP and promotes cancer malignancy. Nat Commun. 2018;9(1):3996.
27. Bedekovics T, Hussain S, Zhang Y, Ali A, Jeon YJ, Galardy PJ. USP24 is a Cancer-Associated ubiquitin hydrolase, novel tumor suppressor, and chromosome instability gene deleted in neuroblastoma. Cancer Res. 2021;81(5):1321–31.
28. Zhi X, Jiang S, Zhang J, Qin J. Ubiquitin-specific peptidase 24 accelerates aerobic Glycolysis and tumor progression in gastric carcinoma through stabilizing PLK1 to activate NOTCH1. Cancer Sci. 2023;114(8):3087–100.
29. Hu Z, Zhao Y, Mang Y, Zhu J, Yu L, Li L, Ran J. MiR-21-5p promotes Sorafenib resistance and hepatocellular carcinoma progression by regulating SIRT7 ubiquitination through USP24. Life Sci. 2023;325:121773.
30. Zhou N, Guo C, Li X, Tu L, Du J, Qian Q, Li J, Huang D, Xu Q, Zheng X. USP24 promotes hepatocellular carcinoma tumorigenesis through deubiquitinating and stabilizing TRAF2. Biochem Pharmacol. 2024;229:116473.
31. Young MJ, Wang SA, Chen YC, Liu CY, Hsu KC, Tang SW, Tseng YL, Wang YC, Lin SM, Hung JJ. USP24-i-101 targeting of USP24 activates autophagy to inhibit drug resistance acquired during cancer therapy. Cell Death Differ. 2024;31(5):574–91.
32. Xiao X, Wang P, Zhang W, Wang J, Cai M, Jiang H, Wu Y, Shan H. GNF-7, a novel FLT3 inhibitor, overcomes drug resistance for the treatment of FLT3–ITD acute myeloid leukemia. Cancer Cell Int. 2023;23(1):302.
33. Shan H, Li X, Xiao X, Dai Y, Huang J, Song J, Liu M, Yang L, Lei H, Tong Y, et al. USP7 deubiquitinates and stabilizes NOTCH1 in T-cell acute lymphoblastic leukemia. Signal Transduct Target Ther. 2018;3:29.
34. Zhang X, Geng L, Tang Y, Wang Y, Zhang Y, Zhu C, Lei H, Xu H, Zhu Q, Wu Y, et al. Ubiquitin-specific protease 14 targets PFKL-mediated Glycolysis to promote the proliferation and migration of oral squamous cell carcinoma. J Transl Med. 2024;22(1):193.
35. Lei H, Xu HZ, Shan HZ, Liu M, Lu Y, Fang ZX, Jin J, Jing B, Xiao XH, Gao SM, et al. Targeting USP47 overcomes tyrosine kinase inhibitor resistance and eradicates leukemia stem/progenitor cells in chronic myelogenous leukemia. Nat Commun. 2021;12(1):51.
36. Abramson J, Adler J, Dunger J, Evans R, Green T, Pritzel A, Ronneberger O, Willmore L, Ballard AJ, Bambrick J, et al. Accurate structure prediction of biomolecular interactions with alphafold 3. Nature. 2024;630(8016):493–500.
37. Siegel RL, Giaquinto AN, Jemal A. Cancer statistics, 2024. CA Cancer J Clin. 2024;74(1):12–49.
38. Yimlamai D, Christodoulou C, Galli GG, Yanger K, Pepe-Mooney B, Gurung B, Shrestha K, Cahan P, Stanger BZ, Camargo FD. Hippo pathway activity influences liver cell fate. Cell. 2014;157(6):1324–38.
39. Juan WC, Hong W. Targeting the Hippo signaling pathway for tissue regeneration and Cancer therapy. Genes (Basel) 2016; 7(9).
40. Moya IM, Halder G. Hippo-YAP/TAZ signalling in organ regeneration and regenerative medicine. Nat Rev Mol Cell Biol. 2019;20(4):211–26.
41. Wu H, Liu Y, Liao Z, Mo J, Zhang Q, Zhang B, Zhang L. The role of YAP1 in liver cancer stem cells: proven and potential mechanisms. Biomark Res. 2022;10(1):42.
42. Liu Z, Li J, Ding Y, Ma M, Chen J, Lei W, Li L, Yao Y, Yu X, Zhong M, et al. USP49 mediates tumor progression and poor prognosis through a YAP1-dependent feedback loop in gastric cancer. Oncogene. 2022;41(18):2555–70.
43. Yan C, Yang H, Su P, Li X, Li Z, Wang D, Zang Y, Wang T, Liu Z, Bao Z, et al. OTUB1 suppresses Hippo signaling via modulating YAP protein in gastric cancer. Oncogene. 2022;41(48):5186–98.
44. Pan B, Yang Y, Li J, Wang Y, Fang C, Yu FX, Xu Y. USP47-mediated deubiquitination and stabilization of YAP contributes to the progression of colorectal cancer. Protein Cell. 2020;11(2):138–43.
45. Zhu H, Yan F, Yuan T, Qian M, Zhou T, Dai X, Cao J, Ying M, Dong X, He Q, et al. USP10 promotes proliferation of hepatocellular carcinoma by deubiquitinating and stabilizing YAP/TAZ. Cancer Res. 2020;80(11):2204–16.
46. Luo H, Jing B, Xia Y, Zhang Y, Hu M, Cai H, Tong Y, Zhou L, Yang L, Yang J, et al. WP1130 reveals USP24 as a novel target in T-cell acute lymphoblastic leukemia. Cancer Cell Int. 2019;19:56.
47. Cao J, Wu S, Zhao S, Wang L, Wu Y, Song L, Sun C, Liu Y, Liu Z, Zhu R, et al. USP24 promotes autophagy-dependent ferroptosis in hepatocellular carcinoma by reducing the K48-linked ubiquitination of Beclin1. Commun Biol. 2024;7(1):1279.
48. Zhang S, Zhou D. Role of the transcriptional coactivators YAP/TAZ in liver cancer. Curr Opin Cell Biol. 2019;61:64–71.
49. Leonardi GC, Candido S, Cervello M, Nicolosi D, Raiti F, Travali S, Spandidos DA, Libra M. The tumor microenvironment in hepatocellular carcinoma (review). Int J Oncol. 2012;40(6):1733–47.
50. Halder G, Dupont S, Piccolo S. Transduction of mechanical and cytoskeletal cues by YAP and TAZ. Nat Rev Mol Cell Biol. 2012;13(9):591–600.

Publisher's note